RTILs as a Matrix in ME-SIMS

May 8, 2006

Christopher Brittin
Advisor: Dr. William E. Cooke
The College of William & Mary

Contents

Abstract

Matrix-enhanced secondary ionization mass spectrometry (ME-SIMS) is a technique used for the molecular analysis of biomaterials. It combines the analysis techniques of time-of-flight secondary ionization mass spectrometry (ToF-SIMS) with sample preparations similar to those used in matrix assisted laser desorption ionization (MALDI). This report addresses two issues: the sample morphology of the solid "crystalline" matrix 2,5 dihydroxybenzoic acid (2,5 DHB) caused by ToF-SIMS, and the potential use of room temperature ionic liquids (RTILs) as a matrix for ME-SIMS. Concerning the former, it was observed that surface degradation of the 2,5 DHB is caused by the vacuum and high voltage which are used in ToF-SIMS. Furthermore, this degradation is difficult to characterize. Concerning the latter, this report will present methodologies which were initially developed to implement RTILs in ToF-SIMS analysis, and some interesting problems which arise from SIMS analysis on RTILs will also be discussed. Finally, this report will present novel techniques which can induce the migration of charged particles within the RTIL.

1 Introduction

Mass Spectrometry (MS) has been critical in the analysis of large biomolecules. Developments in MS techniques, currently allow for sensitive detection of larger fragments of biomolecules. It is hoped that the application of such techniques, especially in the field of "proteomics", will ultimately lead to early disease profiling and non-invasive medical diagnostics [1].

One primary method of MS is secondary ionization mass spectrometry (SIMS). In SIMS, the sample surface is bombarded by energetic primary ions giving rise to secondary ions sputtered from the sample that are detected by a mass spectrometer. Within the past two decades, there has been an increasing number of studies which have attempted to extend the performance of SIMS techniques. One outcome has been the implementation of matrix enhanced SIMS (ME-SIMS). In ME-SIMS, biomolecules are placed in a matrix, which has traditionally been a solid crystal. The use of the matrix increases the mass range of molecules that can be detected by SIMS [6]. However, there are disadvantages associated with solid "crystalline matrices". These matrices cocrystallize with the analyte, producing a heterogeneous sample that gives rise to low signal reproducibility [13, 14]. In addition, the surface topography of a matrix affects the ion yield and the degree of ion fragmentation [2]; therefore, SIMS measurements must takes this into account. The problem is that when a matrix is placed in a SIMS apparatus the surface topography can drastically change. As this paper will show, surface deterioration can arise from high vacuum and out-gassing of the matrix. Furthermore, these changes in the surface topography are extremely difficult to characterize.

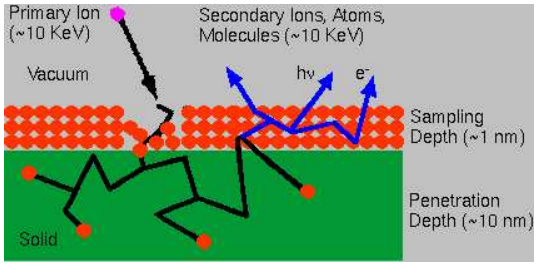

Figure 1: An example of the sputtering that occurs during ion bombardment in SIMS. Taken from [3].

A promising alternative to solid "crysatilline" matrices is room temperature ionic liquids (RTILS). As the name suggests, RTILs are liquids which are thermally stable over a wide range ($\sim$300^{o}C) and have a negligible vapor pressure. The liquid state of the RTIL allows for constant replenishment of the surface. Studies have reported higher signal intensity, better sensitivity, improved sample homogeneity, and therefore better signal reproducibility when RTIL is used as a matrix for matrix assisted laser desorption ionization (MALDI), another popular method of MS [12, 14, 15].

This report will address two subjects. First, the surface morphology of solid "crystalline" matrices caused by ToF-SIMS analysis will be presented. This surface morphology, which will be clear from the data, is extremely difficult to characterize. Second, RTILs will be presented as a potential matrix for ME-SIMS. In doing so, the following will be discussed: initial methodologies developed in order to use RTILs in SIMS measurements and interesting problems which arise when SIMS measurements are attempted on the RTIL. Finally, novel techniques which can be used to induce the migration of charged molecules within the RTIL will be presented.

2 Secondary Ionization Mass Spectrometry

Secondary ionization mass spectrometry (SIMS) is a technique used for mass analysis. Energetic primary ions bombard the surface of a sample causing secondary ions to be sputtered from the surface (Fig.1). This sputtering allows surface molecules to be ejected into a vacuum towards the detector where a spectrum of the secondary ions versus the mass is generated [4].

2.1 SIMS Theory

The ion interaction with surface molecules has been the subject of much research. Using molecular dynamics simulations, Delcorte *et al.* have been able to provide insight into the interactions that generate high yield events [5]. In general, these events occur when the energy of the primary particle is dissipated within the top few monolayers of the sample surface. Through high energy collisions, momentum is transferred to small subsets of atoms

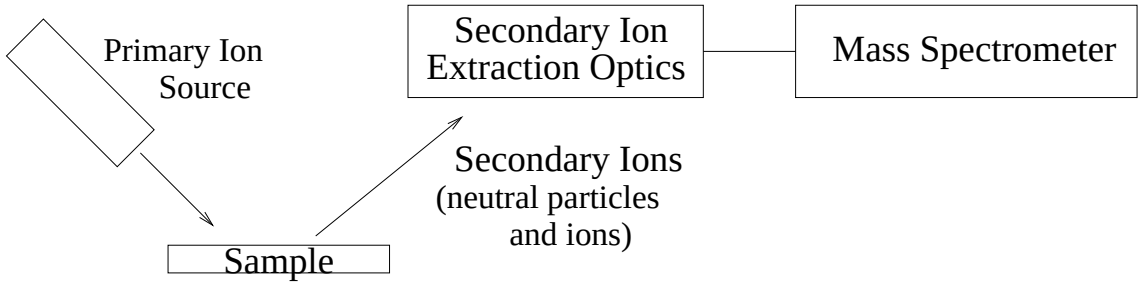

Figure 2: Typical setup for SIMS.

which in turn is distributed to the surrounding volume. This gives rise to subcascades which, when overlapping, create a high energy density inducing the simultaneous motion of many atoms in the excited volume. The excited region then begins to expand and cool causing material to be ejected from the surface.

There are two distinct classes of SIMS technique: dynamic and static SIMS. Dynamic SIMS uses an intense primary ion beam which erodes the surface at sputtering rates of 0.1 to 10 nm/s. The high sputter rates produce elemental ions or low-mass cluster ions. Dynamics SIMS has a high detection sensitivity (parts-per-million to parts-per-billion) and is used in elemental analysis of material science. In contrast, static SIMS uses a low intensity primary ion beam which sputters the top monolayer of the surface. This gives rise to secondary ions which are typically molecular and molecular fragments [6]. Static SIMS will be the focus of this report and more information will follow.

2.2 SIMS Setup

In general, all SIMS apparatuses consist of the same basic components. Figure 2 is a diagram of a general SIMS set-up. The set-up begins with the primary ions. This includes the primary ion source which can vary depending on the type of ion yield desired (positive or negative ions). Typical sources include O_2, Cs, and recently Au. Ion beams are accelerated with a wide range of energies (1 to 25 keV) with a beam diameter that can vary on micrometer scale. Samples are placed in a sample holder within a UHV chamber which minimizes the contamination of the surface. Secondary ions are transported from the surface to the mass spectrometer in a vacuum using electrostatic lenses and apertures [4]. The type of mass spectrometer used varies, but the focus here will be the time-of-flight (ToF) mass spectrometer.

3 ToF-SIMS

Time of flight secondary ionization mass spectrometer (ToF-SIMS) uses ToF analyzers to detect the ejected particles from SIMS. Figure 3 shows a general ToF-SIMS setup. The ejected ions are accelerated by an electric field from a region of length s into a drift chamber

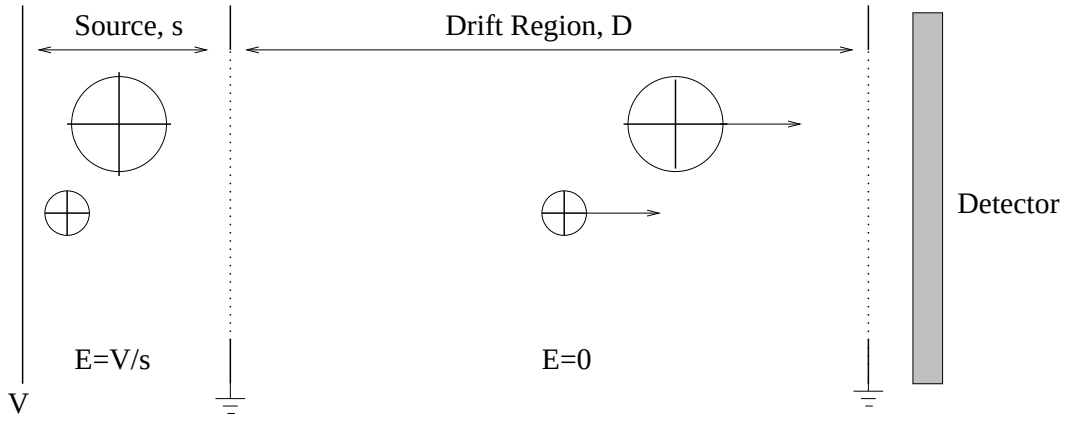

Figure 3: Typical set-up for the ToF-SIMS time of flight analyzer [7].

of length D. The time, t, it takes an ion of charge z to traverse the drift chamber when accelerated by an electric field E can be expressed as follows

$$t = \left(\frac{m}{2zE}\right)^{\frac{1}{2}} D = \left(\frac{ms}{2zV}\right)^{\frac{1}{2}} D \tag{1}$$

where m is the mass of the particle and V is the potential difference in region s. With this mass to charge ratio, the surface composition can be characterized.

ToF-SIMS is versatile and can analyze almost any kind of surface. Analysis is limited to the top few monolayers (~ 10 $\mathring{A}$). The high detection sensitivity (as low as ppm to ppb) is due to its parallel detection of all sputtered ions and its ability to focus the primary ion beam which provides submicrometer lateral resolution [5]. The typical mass resolutions ($M/\Delta M$, full width at half-maximum) in these systems is in excess of 10,000. This is due to the high ion transmission efficiencies of the ion optics used in these systems [6].

4 Matrix Assisted Laser Desorption Ionization

Matrix assisted laser desorption (MALDI) is another technique used in surface characterization. Sample preparations require the formation of crystalline solids out of an aqueous solution, the matrix, and the incorporation of the material to be studied, the analyte, into the matrix crystals. A laser is then used to ablate the molecules in the surface of the sample, thereby ejecting the particles which are detected by a ToF analyzer.

Various investigations of the fundamental desorption and ionization process in MALDI have been performed [8, 9, 10]. A diagram of the MALDI process is shown in Fig. 4. The irradiation of the laser by the matrix gives rise to a plume of ions and neutral fragments. It is generally accepted that ionization occurs during this gas phase, where collisions within the expansion plume creates a supersonic jet of ions and neutrals [6].

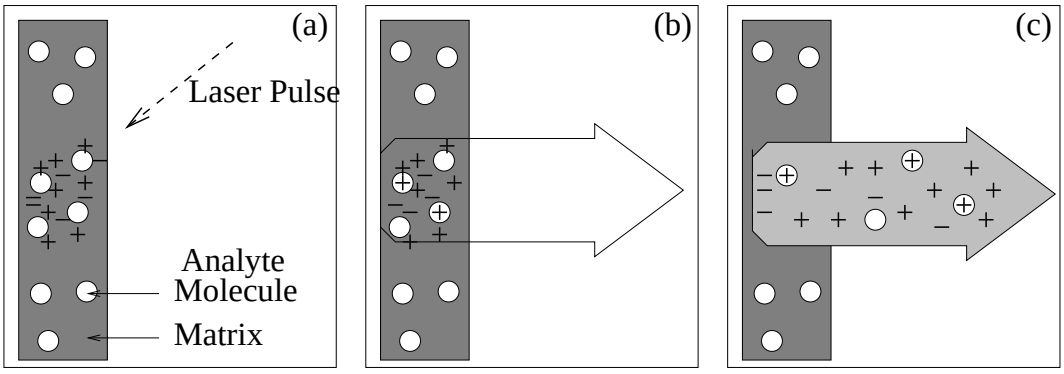

Figure 4: Diagram of the MALDI process: a)Matrix absorbs UV radiation from the laser; b)Matrix begins to dissociate creating a phase change of the matrix to a super compressed gas; c) Matrix expands at a supersonic velocity and analyte is entrained in the expanding matrix plume. Collisions within the plume ionize the analyte molecules. Taken from [7].

5 Matrix Enhanced SIMS

Matrix enhanced secondary ionization mass spectrometry (ME-SIMS) extends the capabilities of both ToF-SIMS and MALDI. ToF-SIMS has a limited mass range due to large biomolecules (greater than 1,000 amu) fragmenting during analysis. This mass range is extended in MALDI through the use of the matrix which creates a nestled environment for the analyte molecules, where molecules well above 200,000 amu have been detected. However, the detection sensitivity of MALDI is limited by the spot size of the laser, typically around 100 μm. ME-SIMS combines these two methods by performing static ToF-SIMS analysis on samples prepared with MALDI protocols [6].

Ionization in ME-SIMS differs from MALDI. Under typical SIMS conditions, only 10 to 100 secondary ions are generated for every 10^5 primary ions. These are not enough secondary ions to facilitate plume interaction. Thus, it is believed that the ions detected by the ToF analyzer are not ionized during or after primary ion impact, rather they are already ionized while still embedded within the matrix [6]. This is why matrices like 2,5 DHB, which have many donor protons, create the highest ion yields in ME-SIMS.

6 Instability of 2,5 DHB in ToF-SIMS

The matrix 2,5 Dihydroxybenzoic Acid (2,5 DHB) was chosen because of studies reporting its high ion yield as a matrix for ME-SIMS [6]. Sample preparations were adopted from existing MALDI protocols [6]. The 2,5 DHB was purchased from Acros Organics (Morris Plains, NJ) and used without further purification. The 2,5 DHB solvent was dissolved in a 50% H_20 and 50% acetonitrile solution to a concentration of $\sim$0.5 M. Other methods of dissolving the DHB solvent were tested in the hopes of producing smoother and more stable crystals (e.g. heating the solution, adding trifluoric acid, and substituting methanol for acetonitrile).

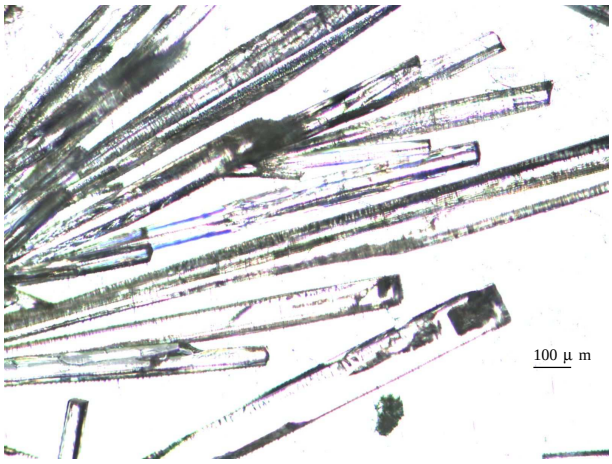

Figure 5: An example of crystals formed on a Ag foil substrate. The bar represents 100 μm.

However, these other methods were found to be worse or not significantly different from the previously stated method.

Once the solution was made, droplets were then pipetted onto a sample substrates and allowed to evaporate forming crystals prior to insertion into vacuum. Substrates were ~ 1 cm^2 silicon chips, chosen for its its flatness [6]. Crystal structures and patterns varied in size, smoothness, and arrangements (Fig. 5) In addition, the individual topography of many single crystals was highly irregular. However, at times smooth nanometer areas could be found.

6.1 Surface Analysis

Surface analysis was carried out at the Applied Research Center in Newport News, VA. Images of the crystals were captured using the Hirox KH-3000VD High Resolution Digital-Video Microscopy System digital microscope. These images were used to visually check for surface degradation (i.e. the relative smoothness of the surface of the crystals) before and after an experiment. However, to gain a depth profile of the surface an atomic force microscope was used (AFM).

6.1.1 Atomic Force Microscope

The atomic force microscope (AFM) is a precision instrument used for surface analysis. The AFM uses a nanometer scale tip located on a cantilever. The cantilever is attached to a piezoelectric material. By applying a voltage to this material, the AFM is able to make scans in the (x, y) plane. At each (x, y) point the vertical displacement of the tip is recorded. Light from a laser diode is reflected off the cantilever and collected by a position sensitive detector (PSD)(Fig. 6). The PSD consists of two photodiodes and the output signal, which is proportional to the angular displacement of the cantilever, is collected by a differential amplifier (Fig. 7).

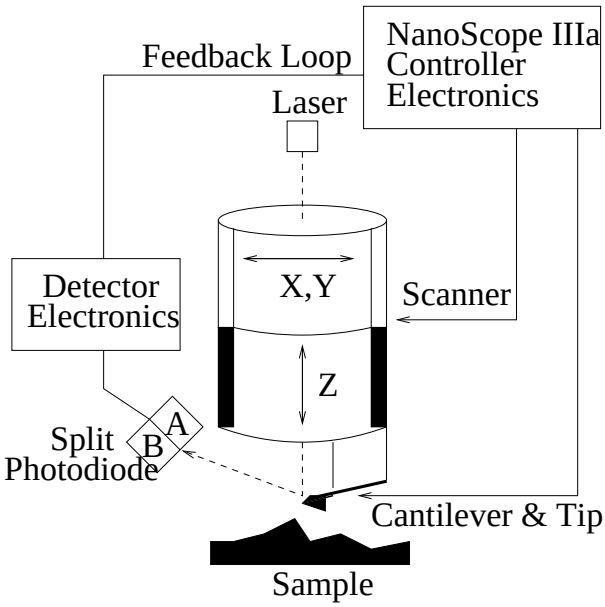

Figure 6: Diagram of the AFM. The AFM operates in "tapping mode". The feedback loop maintains the constant oscillation amplitude of the cantilever. The vertical position at each (x,y) data point is stored by the computer to form a topographic image.

The AFM was operated in "tapping mode". In this mode, the cantilever oscillates at or near resonance (∼250 kHz) and records the height of the surface when the tip touches on each downward stroke. Operating in this mode minimizes distortion from drag and reduces the wear on the tip [17]

6.1.2 Initial images

Prior to placing the crystals in a SIMS environment, HIROX and AFM images were taken of the matrix surfaces. Atomically flat or near flat areas (±1 nm)were located using the AFM. The AFM tip was then used to scratch the surface (Fig. 8). By marking the surface in this manner, the same area could be analyzed following ToF-SIMS, allowing for before and after comparisons of the matrix.

6.1.3 Primary Analysis

Experiments were then performed at William & Mary in order to isolate the damage caused by vacuum from the damage caused by an applied voltage. All matrices were placed in a vacuum which was allowed to pump down to 10^{-7} torr. While under vacuum, a +5 kV and a -5 kV potential were applied to separate matrices for 30 minute while one matrix remained grounded during this duration. Following this, optical images and AFM images were taken and compared with the initial images.

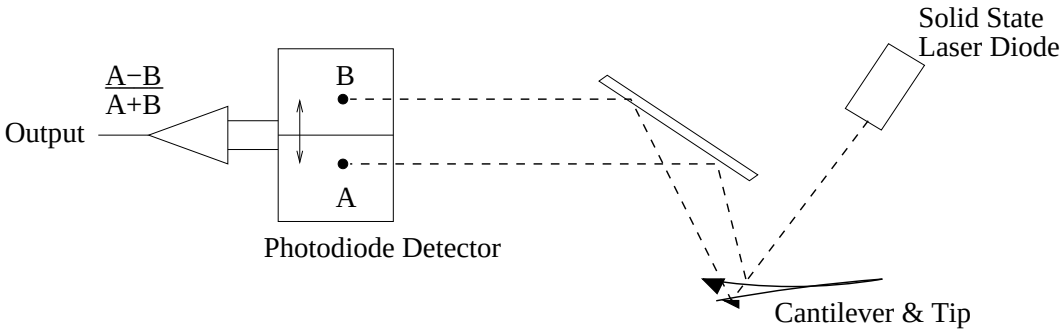

Figure 7: The PSD of the AFM. Light is reflected off the cantilever and collected by a PSD. The PSD consists of two photodiodes and the output signal is collected by a differential amplifier. The angular displacement of the cantilever is proportional to the output signal: $\frac{A-B}{A+B}$.

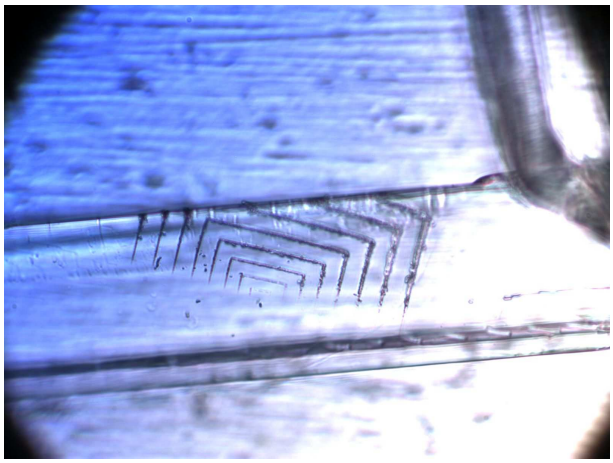

Figure 8: Spiral scratch on the crystal surface created with the AFM to ensure that the same area is analyzed before and after placement in the ToF-SIMS. The distance between lines is $\sim 10\mu$m.

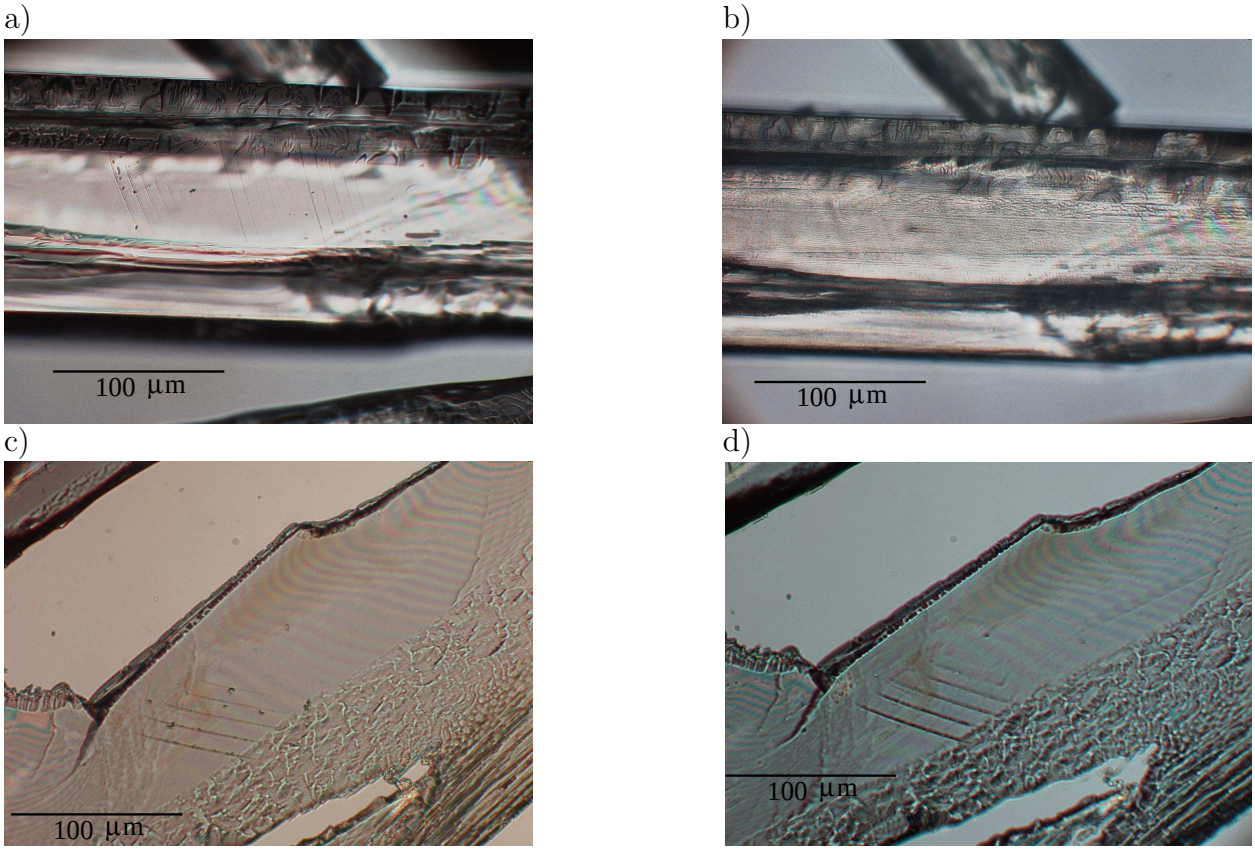

Figure 9: The before (a,c) and after (b,d respectively) images of the sample placed in vacuum ($\sim 10^{-7}$ Torr) but no voltage was applied. The bar represents 100 μm.

6.2 Results

The following results are from two separate experiments performed on the 2,5 DHB. Figures 9-11 include optical images before and after the crystals were exposed to vacuum and an applied voltage. Figure 9 was grounded while in vacuum. Figure 10 was exposed to -5 kV voltage while in vacuum. Figure 11 was exposed to a +5 kV voltage while in vacuum.

Figures 12-14 are the respective 3-D images for the previous figures (9-11) generated by the AFM. All images are 15 μm $\times$ 15 μm, with a vertical scale of 300 nm.

6.3 Discussion

Analysis on the 2,5 DHB crystals is ultimately inconclusive. It was hoped that this experiment would be able to isolate the damage caused by vacuum from the damage caused by the applied voltage. However, not only were the results not reproducible, but it appears that a large amount of the surface degradation can be attributed to vacuum.

Consider images for the crystals placed just in vacuum. Figure 12 b) shows extensive surface degradation while figure 12 d) shows some alteration to the surface but certainly not

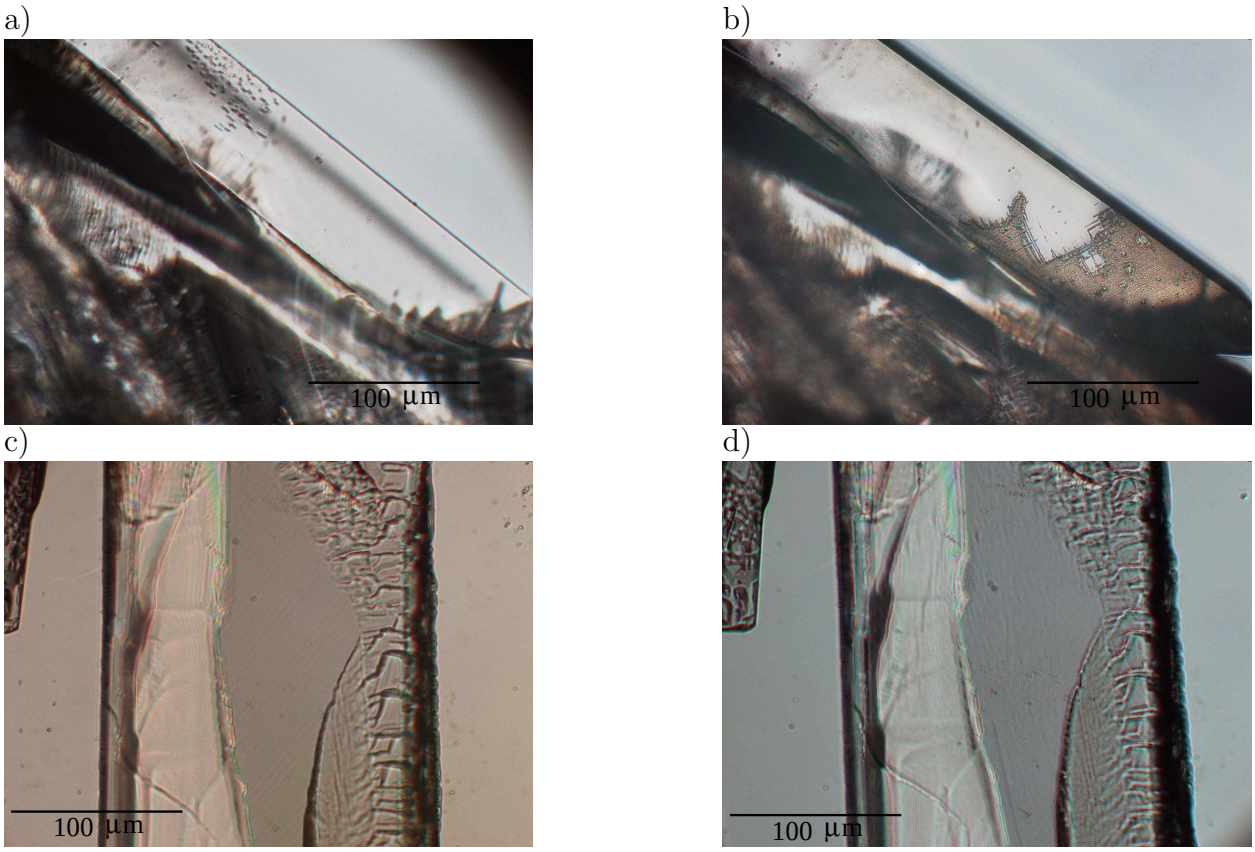

Figure 10: The before (a,c) and after (b,d respectively) images of the sample placed in vacuum ($\sim 10^{-7}$ Torr) with -5 kV applied for 30 minutes. The bar represents 100 μm.

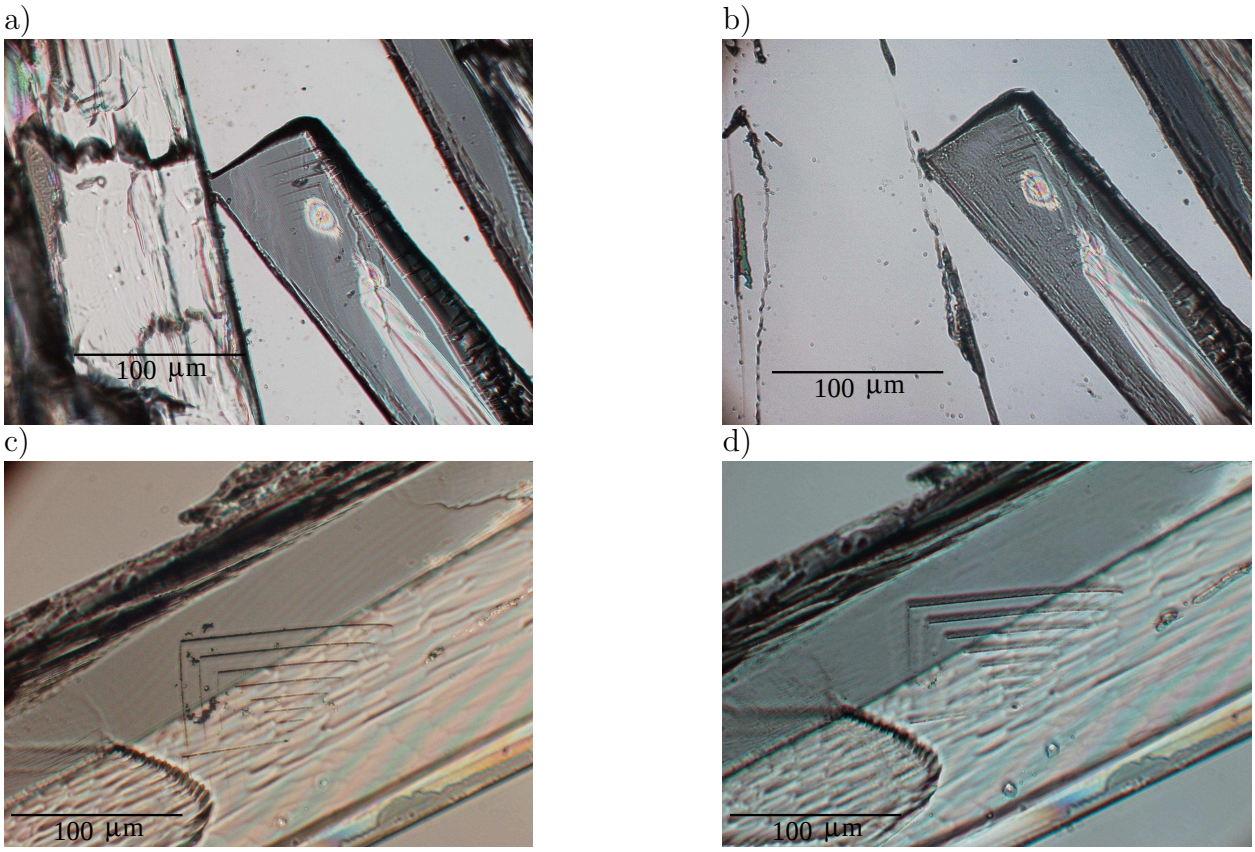

Figure 11: The before (a,c) and after (b,d respectively) images of the sample placed in vacuum ($\sim 10^{-7}$ Torr) with +5 kV applied for 30 minutes. The bar represents 100 μm

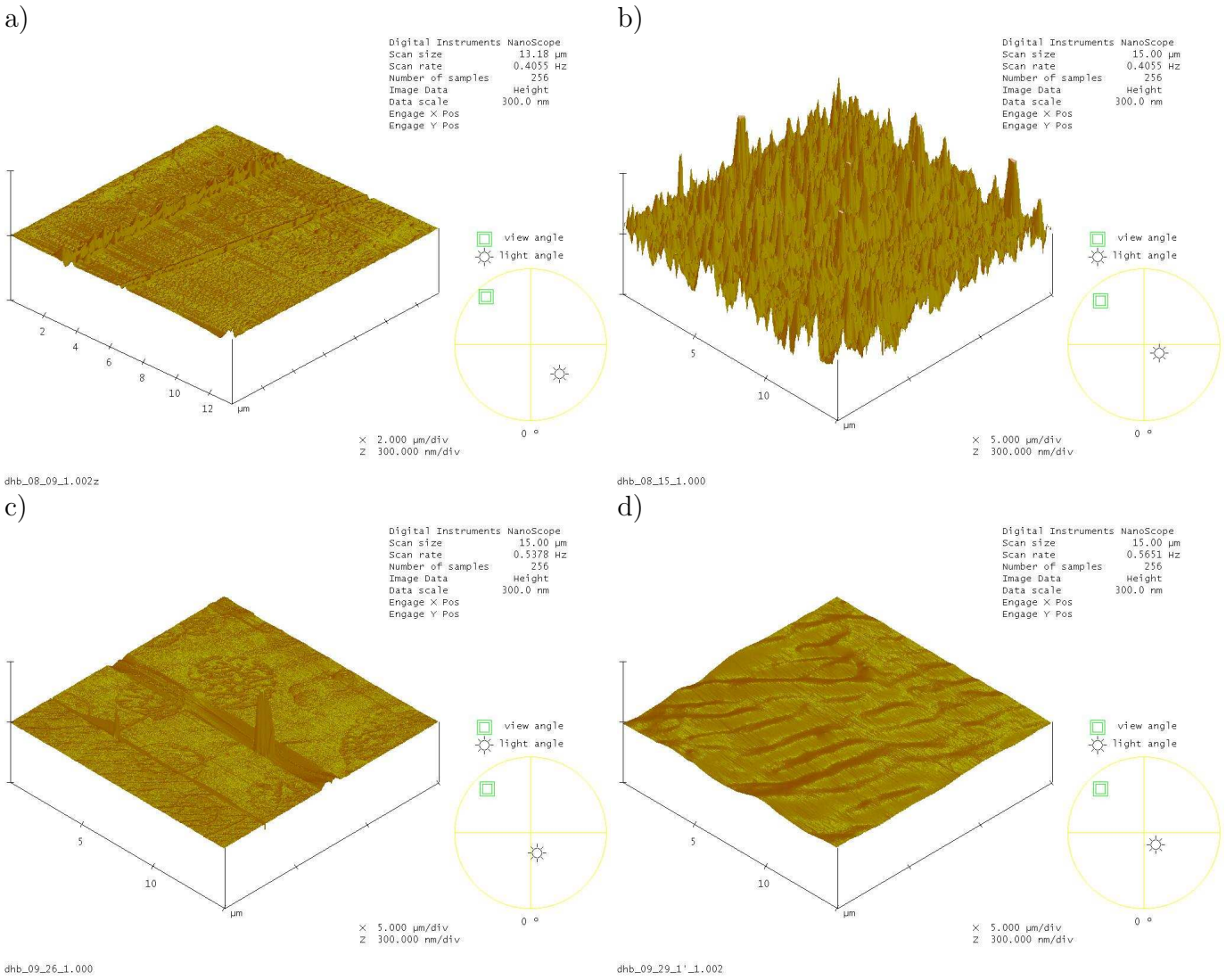

Figure 12: The before (a,b) and after (b,d respectively) AFM images of the sample placed in vacuum ($\sim 10^{-7}$ Torr) but with no voltage applied. All images are 15 μm $\times$ 15 μm, with a vertical scale of 300 nm.

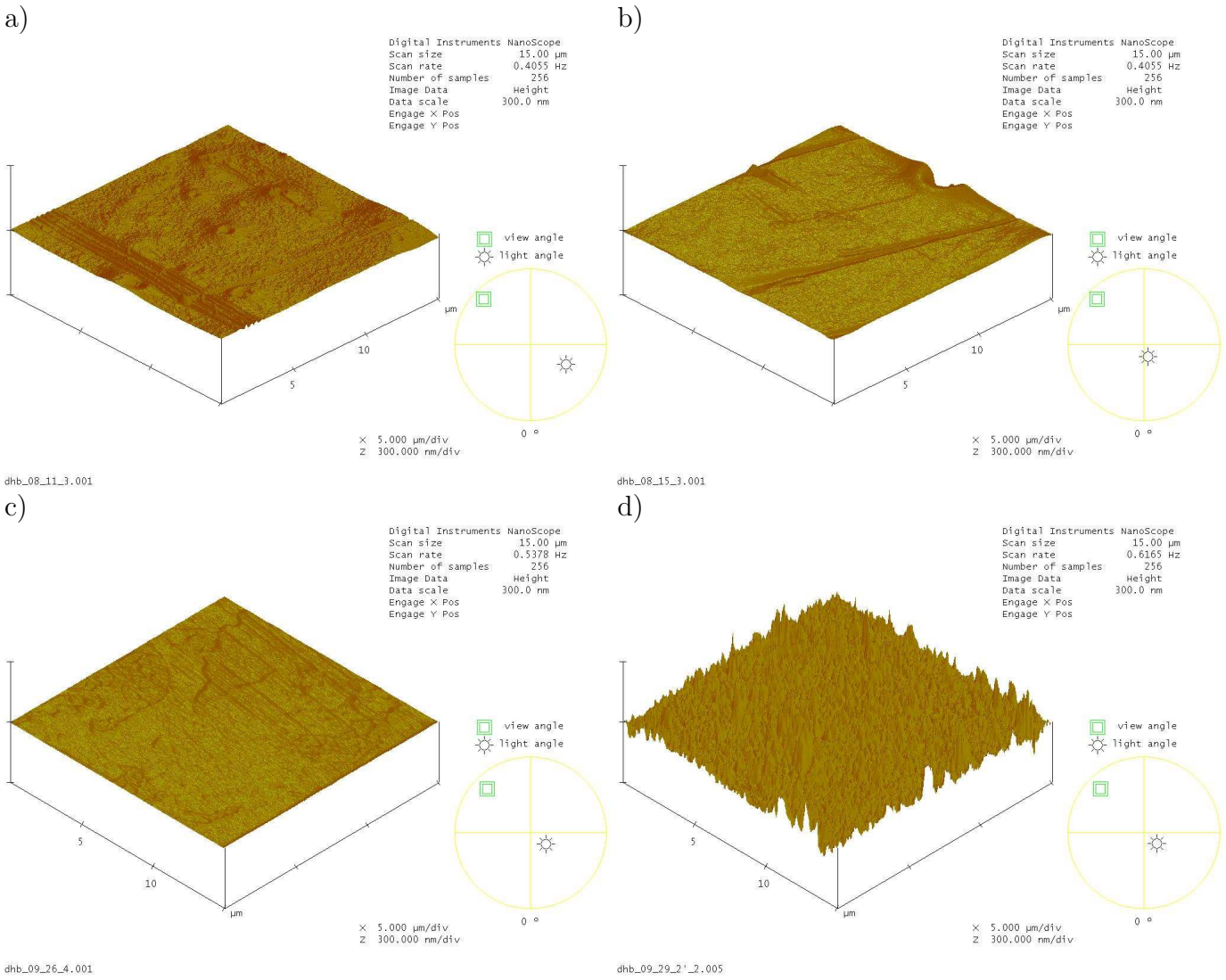

Figure 13: The before (a,c) and after (b,d respectively) AFM images of the sample placed in vacuum ($\sim 10^{-7}$ Torr) with -5 kV applied for 30 minutes. All images are 15 μm $\times$ 15 μm, with a vertical scale of 300 nm.

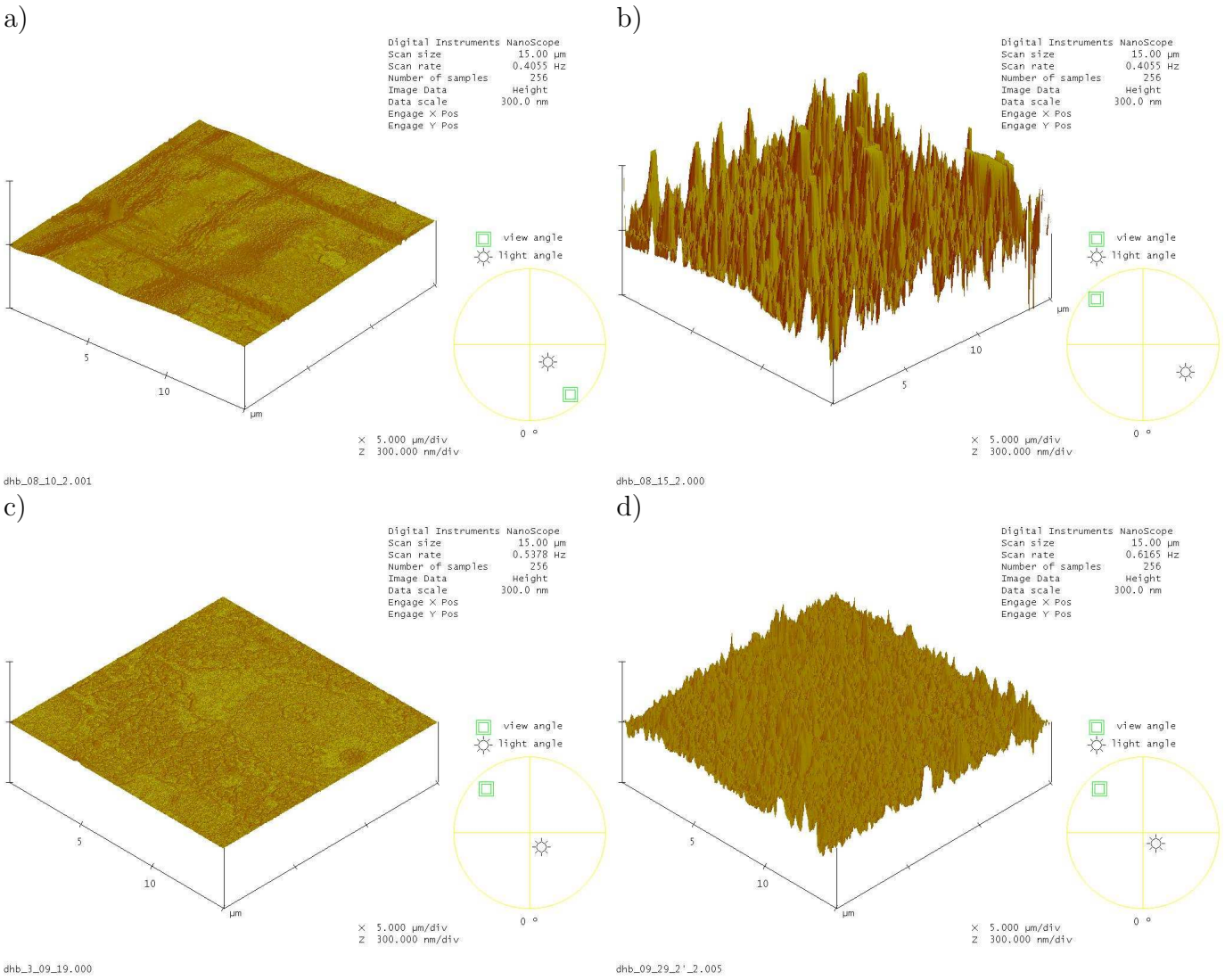

Figure 14: The before (a,c) and after (b,d respectively) AFM image of the sample placed in vacuum ($\sim 10^{-7}$ Torr) with +5 kV applied for 30 minutes. All images are 15 μm $\times$ 15 μm, with a vertical scale of 300 nm.

as extensive. The damage caused by the vacuum is attributed to two causes: the formation of gas pockets in the crystal created during the evaporation process and the build up of surface charge caused during the pumping down process. However, the former seems more likely given the manner in which the crystals are prepared. The damage caused by vacuum makes it difficult to characterize the damage caused by the applied voltage.

The surface degradation caused by the applied voltage is not clear. In most cases, there appears to be extensive surface degradation. It is not evident whether this is caused by the vacuum or the applied voltage. Figure 13 (b) seems to contradict this by showing no signs of surface degradation. However, comparing this AFM image with the optical image, Fig. 10 (b) which shows extensive visual damage caused to the surface, suggests that the chosen crystal area was an anomaly. Thus, it appears that the 2,5 DHB matrix is extremely unstable and difficult to characterize.

7 RTILs as a Matrix for ME-SIMS.

Room temperature ionic liquids (RTILs) have properties that make their use as a liquid matrix in ME-SIMS very attractive. They possess a thermal stability of over 300^o C and a negligible vapor pressure. RTILs are formed by the association of an anion and a cation. At least one ion has a delocalized charge and one component is inorganic, which prevents a stable crystal lattice from forming [16].

For this study, the RTIL 1-butyl-3-methylimidazalium hexafluorophosphate was used. The RTIL was purchased from Chemada Fine Chemicals Ltd. and was used without further purification. It consists of the cation $[C_5H_{15}N_2]^+$ and the anion $[PF_6]^-$, and has a total molecular weight of 284 g/Mol.

7.1 Stability of RTILs in ToF-SIMS

In an effort to develop a preliminary knowledge of the stability of RTIL in vacuum, the RTIL was applied to the bottom of a plastic petri dish and placed in a vacuum bell jar, which was calculated to have a pressure of $\sim 10^{-7}$ torr. The RTIL was sprayed on with an atomizer at various distances from the petri dish in order to determine if there is a correlation between the size of the droplets and their stability. In addition, the RTIL was mixed with a red laser dye with molecular weight 580.66. This was done in order to make the drops more visible and to determine how the RTIL reacts with foreign substances, information which will be beneficial when proteins are eventually mixed with the RTIL.

Results from the investigation of RTIL stability are presented here. Figures 15, 16, and 17 show images of the RTIL when applied with an atomizer from 3 cm, 15 cm, and 30 cm, respectively, from the petri dish. The RTIL prior to being placed in vacuum is presented on the left while the same area post vacuum is presented on the right. The bar represents 100 μm.

These experiments show that RTILs are extremely stable under high vacuum. Figures 15-17 show that visual changes in the RTIL structure is minimal and decreases as the size

a) b)

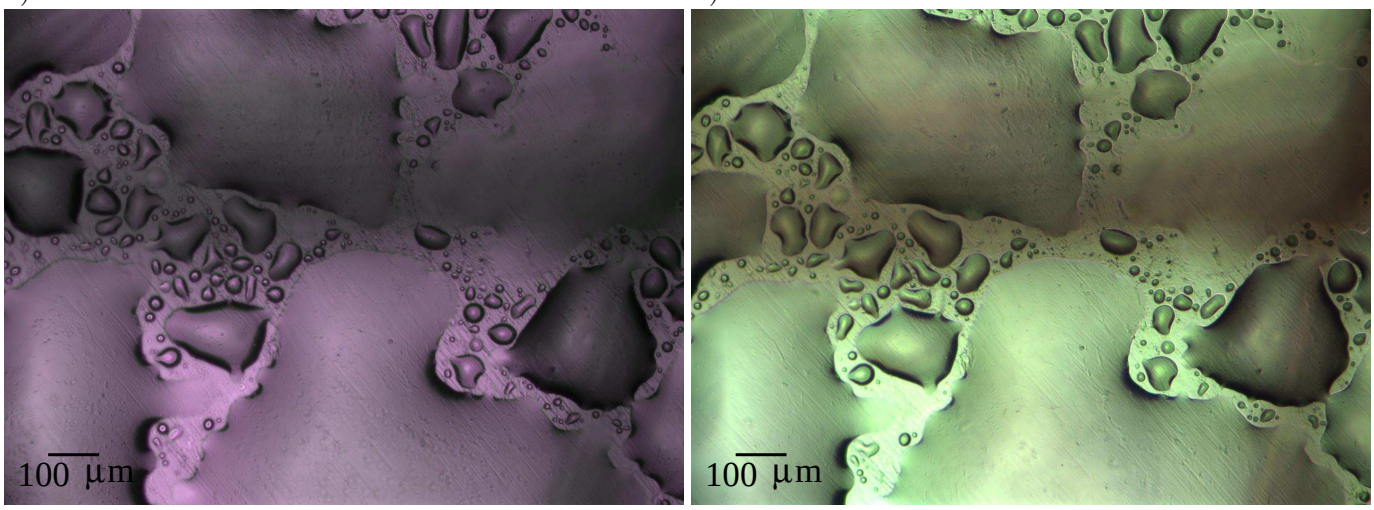

Figure 15: The RTIL when applied with an atomizer at a distance 3 cm from the petri dish bottom. The RTIL was place in a vacuum bell jar at $\sim 10^{-7}$ torr. The RTIL prior to vacuum is presented in a) while the same area post vacuum is presented in b). The bar represents 100 μm.

a) b)

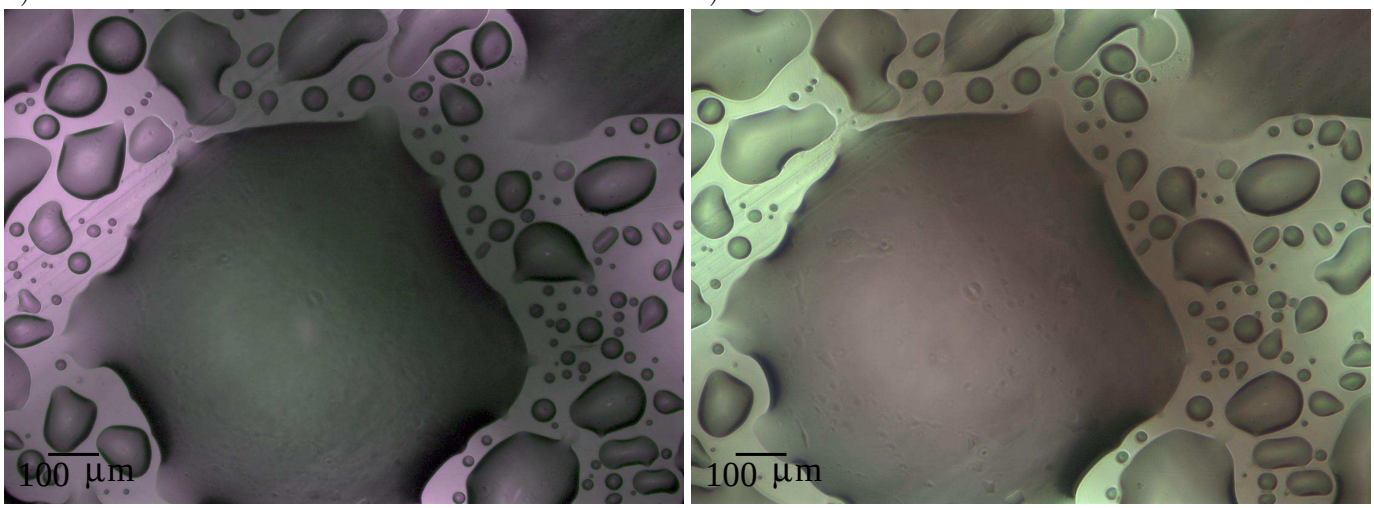

Figure 16: The RTIL when applied with an atomizer at a distance 15 cm from the petri dish bottom. The RTIL was place in a vacuum bell jar at $\sim 10^{-7}$ torr. The RTIL prior to vacuum is presented in a) while the same area post vacuum is presented in b). The bar represents 100 μm.

a) b)

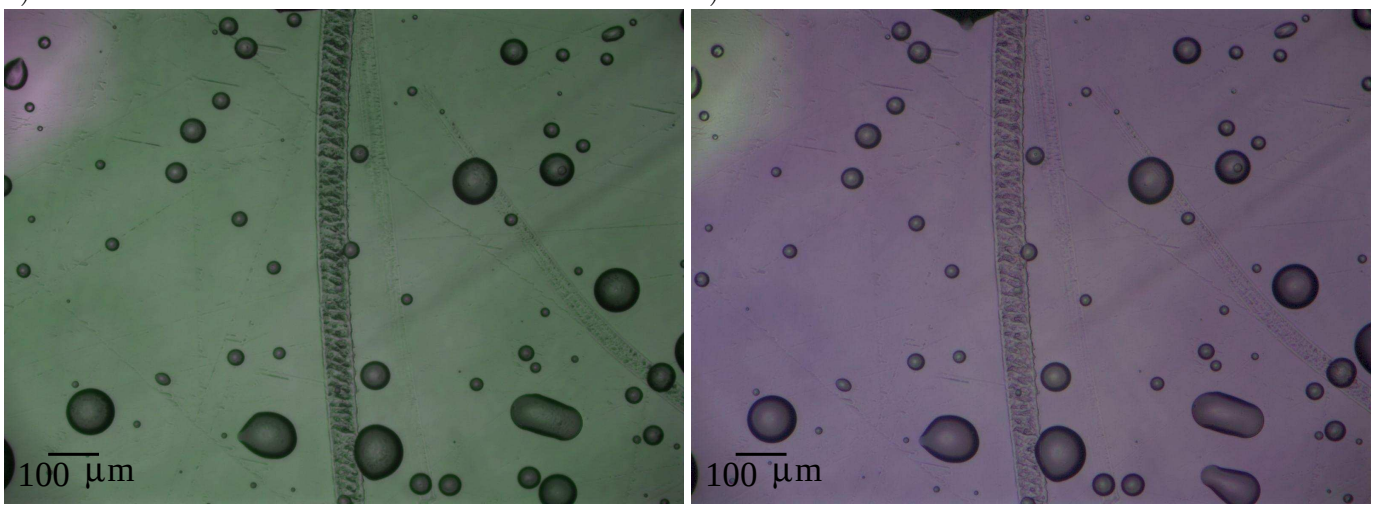

Figure 17: The RTIL when applied with an atomizer at a distance 30 cm from the petri dish bottom. The RTIL was place in a vacuum bell jar at $\sim 10^{-7}$ torr. The RTIL prior to vacuum is presented in a) while the same area post vacuum is presented in b). The bar represents 100 μm.

of the droplets become smaller. This suggests that a negligible amount of volume of RTIL is lost in vacuum.

7.2 RTIL in ToF-SIMS

RTIL droplets were sprayed onto a Au coated silicon substrate using an atomizer. Droplets, on average, had a diameter on the order of 10-100 μm. Optical images of specific drops were generated with the Hirox KH-3000VD High Resolution Digital-Video Microscopy System prior to ToF-SIMS. These specific droplets were then analyzed in the PHI-TRIFT II ToF-SIMS. Data files collected from the ToF-SIMS were then inputted into a MATLAB program, where spectra and chemical images of the droplets were generated. The chemical images show where ToF-SIMS maps the surface ejection of ions from the sample. Additionally, chemical images were generated which displayed only the specific cation or anion of the RTIL, Bmim and PF_6, respectfully.

7.2.1 RTIL Images

The following presents data collected from a specific droplet of RTIL which was measured to have a diameter of 93 μm. The optical image presented in Fig. 18 has been rotated to reflect its orientation when placed in the ToF-SIMS. Figure 19 presents images generated by MATLAB based on the ToF-SIMS data, which display only the cation or anion.

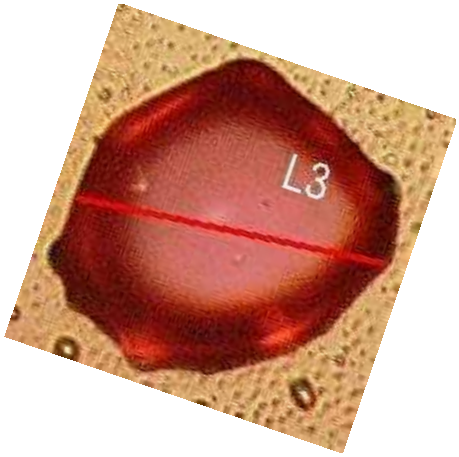

Figure 18: Optical image of an RTIL droplet which had a diameter, measured by the red line, of 93 μm. The image has been rotated to reflect the droplet's orientation in the chemical images which follow.

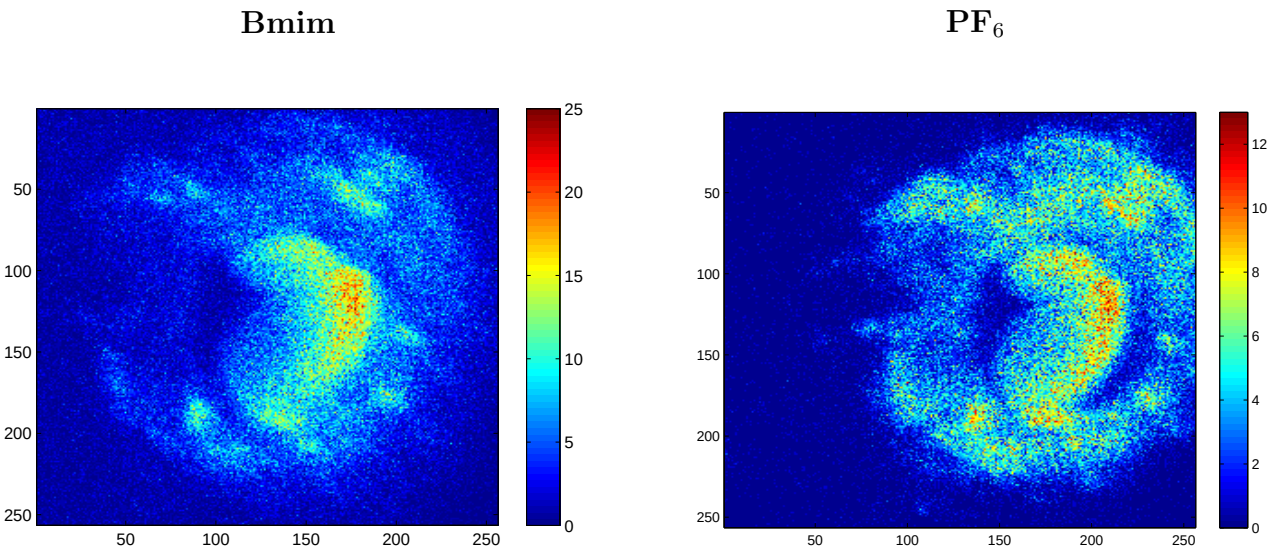

Figure 19: Chemical images of the RTIL in ToF-SIMS generated by MATLAB. The image is a 256×256 pixelated image of data collected by the ToF-SIMS over a raster size of 100 μm. The image shows where ToF-SIMS maps the surface ejection of ions from the RTIL. The brightness of a region is proportional to the intensity of ejected ions. The left image displays only the cation, Bmim, and the right image displays only the anion, PF_6.

7.2.2 Discussion

There is a noticeable "hot spot" which appears on the right side of the droplet in Fig. 19. It was expected that, given the liquid nature of RTIL, the detection of ions would be more uniform, or at the very least any "hot spot" would be concentrated in the center of the surface of the bubble. The reason for the shifted "hot spot" is still uncertain, however there are a few speculations. The first and most likely reason is attributed to the geometry of the RTIL bubble. The ToF-SIMS is designed to analyze essentially flat surfaces. The height of the RTIL bubble could potentially cause a parallax which gives rise to the shift of the "hot spot" from the ToF-SIMS. The second hypothesis for the "hot spot" is that the shift is due to grazing incidence angles between the ToF-SIMS ion beam and the RTIL bubble. Further research must be conducted to determine which hypothesis is correct.

8 Induced Migration of Charged Particles in RTIL

The induced migration of charged particles in RTIL is not a trivial matter to understand. Given the ionic and viscous properties of RTIL, it is not even evident a priori whether such migration can easily be achieved. For example, one could hypothesize that the application of an electric field to the RTIL might cause a build up of ionic charge, which could shield charged analytes within the RTIL. The following experiments will show that this is not the case. Migration can be easily achieved, even if it is not easily understood.

8.1 Experimental Section

In the following experiment, charged dye was mixed with RTIL to model the migration of charged particles. The dye used was bromophenol blue (BB), a dye commonly used in gel electrophoresis. The dye has a slight negative charge and has a molecular weight of 620 g/Mol. BB is a pH indicator and its transition intervals are given in Table 1. The setup for this experiment was as follows. The BB dye was mixed with the RTIL at a concentration of 0.5 mg/mL. Droplets of the mixture were placed in a plastic petri dish, forming one semispherical drop. The drop measured ∼10 mm in the x,y plane and ∼1-2 mm in the z direction (Fig. 20). Two copper electrodes, 100 μm in diameter, were place at opposite sides of the drop. A positive current was then applied to the droplet and migration of the dye was observed. Finally, a negative current was applied and reversal of the migration was observed. The application of a current to the BB-RTIL mixture was important, initial experiments showed that no migration could be achieved with only an applied voltage. Therefore, in the data that follows the voltage that was applied to the RTIL droplet will be stated followed by the current that was measured.

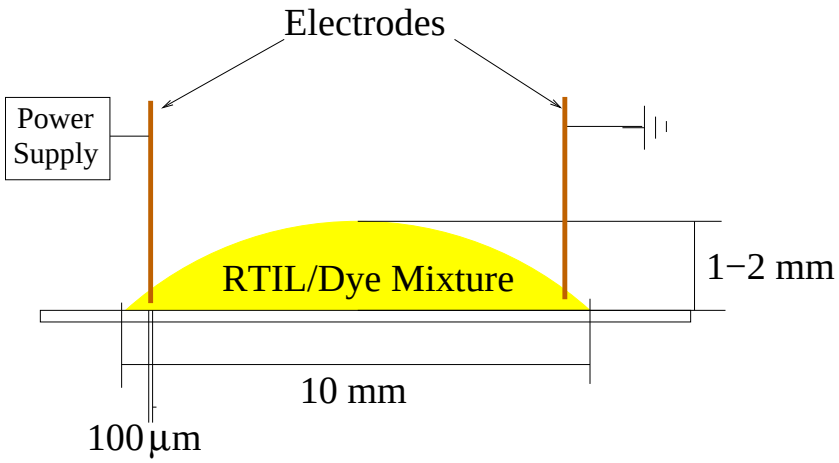

Figure 20: The setup for the induced migration of charged particles within RTIL. A droplet of BB-RTIL mixture (yellow in color due to the pH) was placed at the bottom of a petri dish. Two electrodes were placed in opposite ends of the drops. A current was then applied to the drop.

Bromophenol Blue pH Transitions	
pH	Color
≤ 3.0	yellow
3.4	green
≥ 4.6	blue

Table1: The colors associated with the pH of bromophenol blue solutions.

8.2 Results

Figure 21 shows the affects of applying a current to the BB-RTIL mixture. The positive electrode was located on the left side of the drop while the negative electrode was placed on the right side of the drop. Next the migration of the dye is shown. Figure 22 shows the migration of dye which arose when 4 V was applied to the BB-RTIL mixture with a measured current of 1.4 mA. The positive electrode was located on the left side of the drop while the negative electrode was placed on the right side of the drop. These images were taken over the course of 1 hour. Figure 23 shows the same droplet 0.5 hours after the applied voltage was turned off. Figure 24 shows the migration of dye in the same droplet which arose when - 4 V was applied to the BB-RTIL dye mixture, with a measured current of -1.8 mA. The negative electrode was located on the left side of the drop while the positive electrode was located on the right side of the drop. The images were taken over 2 hours.

a) b)

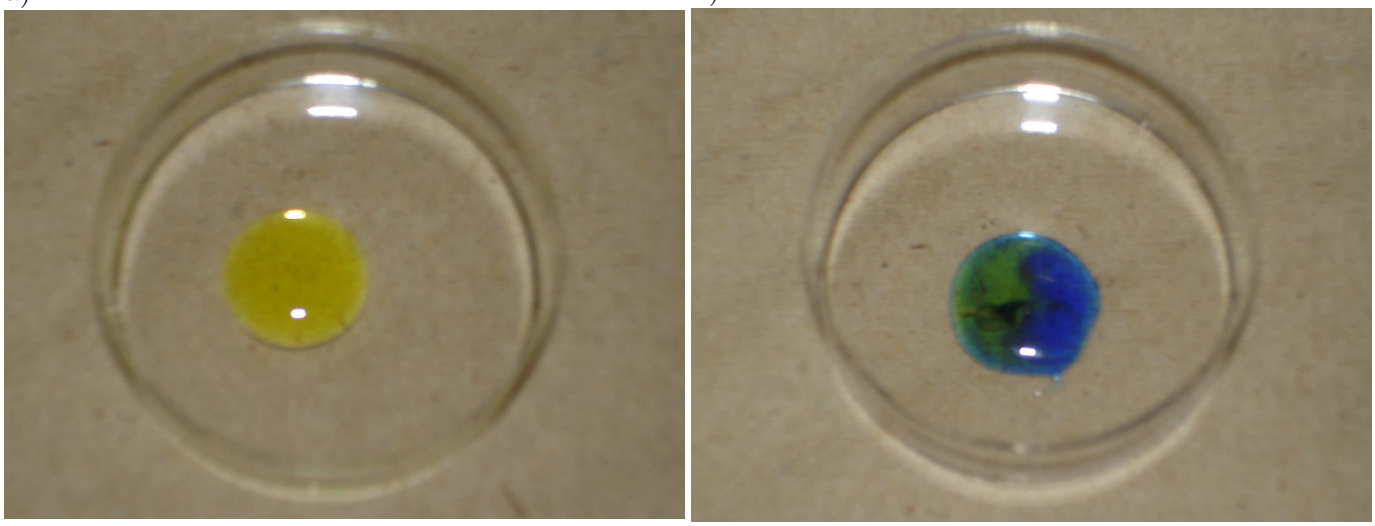

Figure 21: The affect of applying a current to the BB-RTIL mixture. Note that the positive electrode was located on the left while the negative electrode was located on the right. a)The initial yellow color of BB-RTIL mixture. b) The same yellow drop 5 minutes after a voltage had been applied.

a) b)

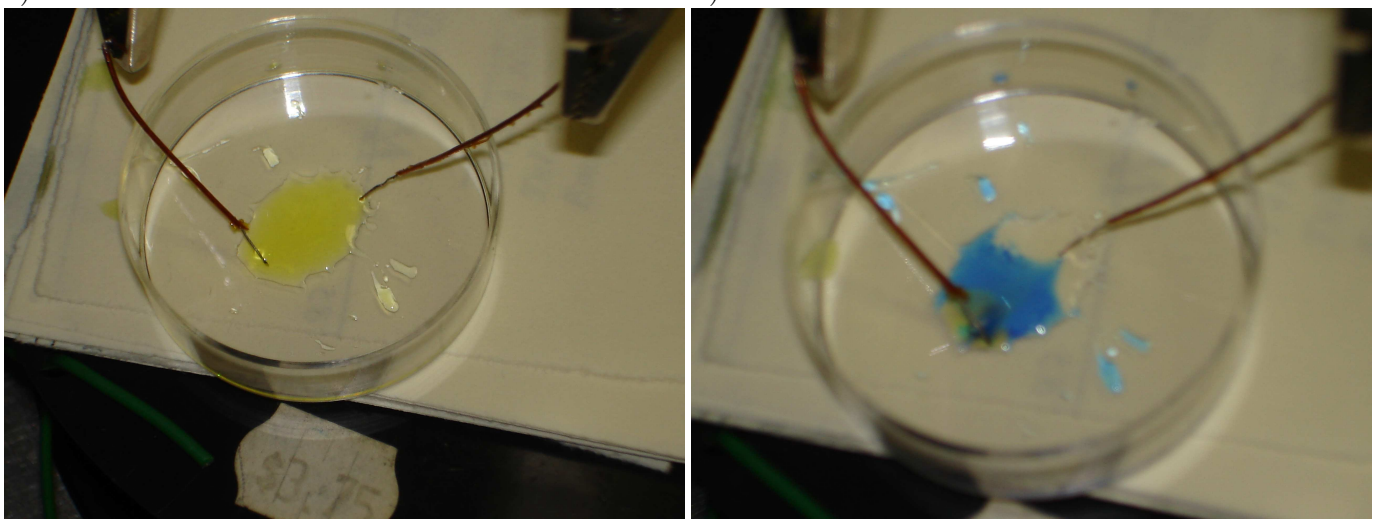

Figure 22: The migration of BB dye in RTIL when 4 V is applied to the left side of the BB-RTIL mixture, with a measured current of 1.4 mA. a)The initial droplet. b) The droplet 1 hour later, with dye migration to the left.

a) b)

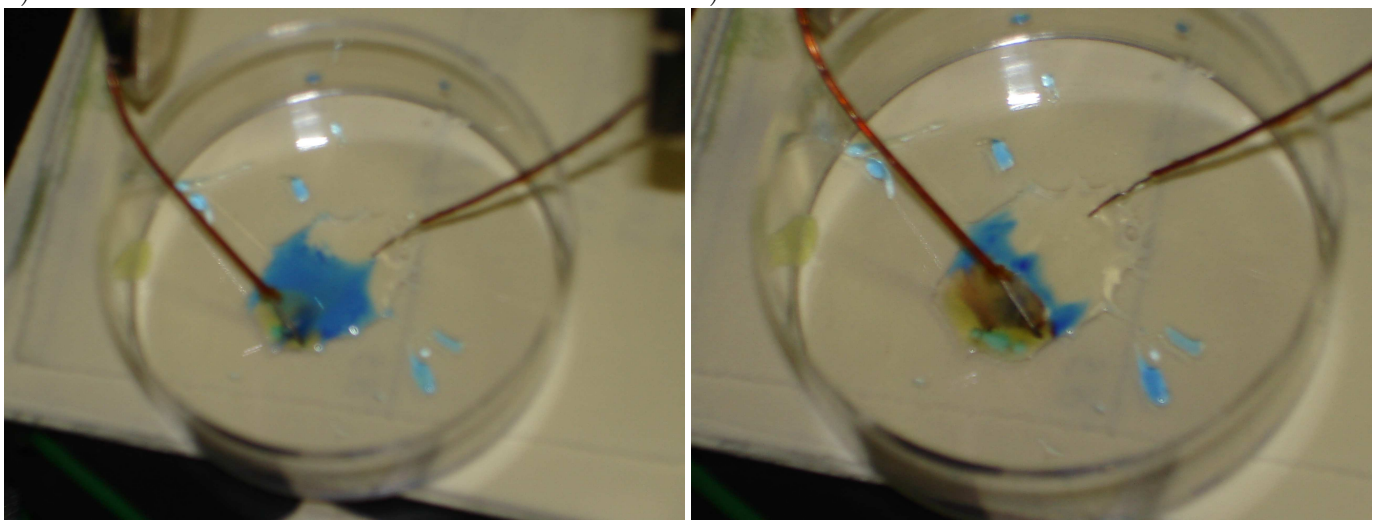

Figure 23: This is a follow up of Fig. 22 after the voltage was turned off. a)The droplet before the voltage was turned off. b) The droplet 0.5 hours after the voltage was turned off, with continued dye migration to the left.

a) b)

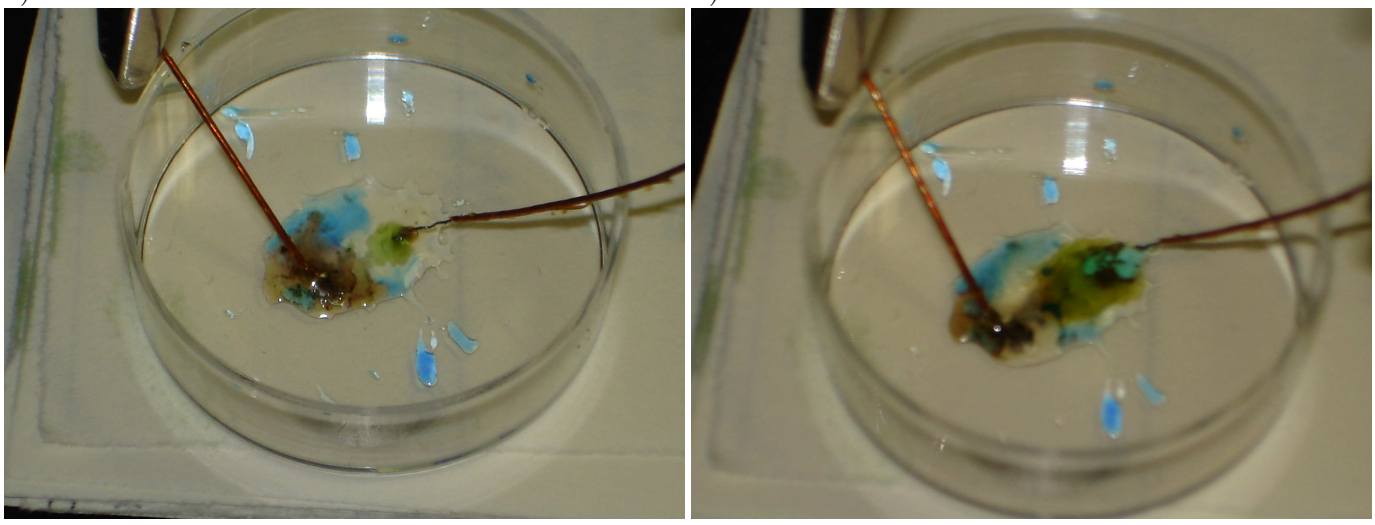

Figure 24: This follow up of Fig. 23 after a voltage of -4 V was applied on left side of the drop, with measured current -1.8 mA. a)The droplet when the negative voltage was initially applied. b) The droplet 2 hours later, with dye migration to the right.

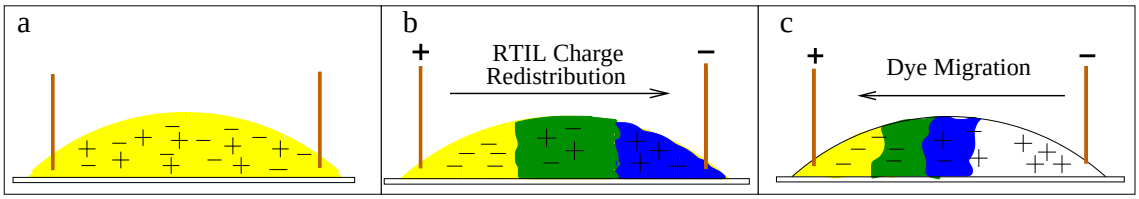

Figure 25: This cartoon shows what happens when a current is applied to the BB-RTIL mixture. a) Initially, both the BB dye and charges of the RTIL are uniformly distributed. b)The positive charges of the RTIL concentrate around the negative electrode. This gives rise to a concentration gradient of charge across the RTIL which is reflected in the pH sensitive color of the BB-RTIL mixture. c) The negative BB dye begins to migrate to the positive electrode.

8.3 Discussion

It is clear that migration of the dye can easily be achieved when a current is applied to the BB-RTIL mixture. However, the process of the migration needs some further explanation and is illustrated in Fig. 25. When a current is initially applied to the BB-RTIL mixture, it causes charges in the RTIL, not the dye, to migrate. This can be seen from Fig. 21. When a positive current was applied to the mixture, the positive charges of the RTIL were attracted to the negative electrode, located on the right side of the drop. This caused the local pH on the right side of the drop to increase, which gave rise to the blue color change of the BB-RTIL mixture in this local region of the drop. Recall from Table 1 that green reflects a lower pH than blue. It appears that the application of a current causes a concentration gradient of charge across the droplet, from left to right.

Either during or immediately following the RTIL's charge redistribution, the dye begins to migrate. This migration is evident in Fig. 22, where the area immediately surrounding the negative (right) electrode became clear after 1 hour, where the blue dye has migrated to the left. Since the dye has a slight negative charge, it was obviously repelled by the negative electrode. Further inspection of Fig. 22 will reveal that the immediate area surrounding the positive (left) electrode has turned yellow. It would appear that the dye began to concentrate around the positive electrode and returned to its initial pH. Figure 23 shows that migration of the dye continues even when the voltage has been turned off. This is most likely due to positive charges within the RTIL which become concentrated on the right side of the drop and continue to repel the negatively charged dye, even when no external current is applied. Figure 24 shows that this migration can be reversed. As can be seen from the images, when the sign of the voltage is switched black spots begin to form. These black spots cannot yet be explained. However, careful inspection shows the yellow region, once around the left electrode, migrates to the right (now positive) electrode. The area around the left electrode becomes the clear RTIL.

9 Conclusion

MS has developed into an important technique in the analysis of large biomolecules. Promising results have been seen in the applications of ME-SIMS, which combines ToF-SIMS analysis with the sample preparation of MALDI protocol. However, whereas extensive studies have been done on the morphology of matrix topographies in MALDI, no such studies have been published for ME-SIMS. SIMS analysis, though not as extensive as MALDI, does vary with surface topography. The characterization of the effects of SIMS analysis on the topography of a matrix would be very beneficial.

The effects of ToF-SIMS analysis on the matrix 2,5 DHB was studied. During ToF-SIMS analysis, DHB crystals are subjected to high vacuum and an applied voltage. It was found that a large amount of surface degradation was caused by vacuum alone. This surface degradation is difficult to characterize and prevents the characterization of other parameters (e.g. the applied voltage and the use of the ion beam on the crystal). The degradation caused by the vacuum is attributed to the release of gas pockets in the crystal during vacuum. The inability to characterize the degradation of this solid "crystalline" matrix led to the consideration of an alternative liquid matrix.

RTILs offer many potential benefits for ME-SIMS. They are both thermally stable and have a negligible vapor pressure. Studies have reported RTILs having higher signal intensity, better sensitivity, and better signal reproducibility when compared to solid matrices. This report was able to show that the specific RTIL, 1-butyl-3-methylimidazalium hexafluorophosphate, is indeed stable in a SIMS environment (i.e. high vacuum). Furthermore, a methodology using an atomizer was developed which could successfully implement a RTIL matrix into ToF-SIMS. Currently, other methodologies are being explored, such as spin coating.

The ToF-SIMS analysis of the RTIL presented some interesting problems. There was a noticeable "hot spot" which was shifted to the right of the bubble. The shifted "hot spot" could be attributed to a parallax which arises from the geometry of the bubble. However, other reasons such as grazing incidence angles between the ToF-SIMS ion beam and the RTIL bubble have not been completely ruled out. Currently, substrates are being designed which will place the RTIL at different incidence angles relative to the ion beam of ToF-SIMS. Any noticeable shift in the "hot spot" with the change in the incidence angle would support the hypothesis that ToF-SIMS is sensitive to grazing incidence angles.

Finally, the induced migration of charged particles within the RTIL was studied. It was shown that when a current is applied to the BB-RTIL mixture, charged particles could easily be caused to migrate within the RTIL. Initially when a current is applied, the charges within the RTIL redistribute themselves and form a concentration gradient that reflects the applied current. During this charge redistribution, or immediately following, migration of the charged dye begins to occur. This process can also be reversed. Further studies must be done to see if this process can be extended to biomolecules within the RTIL. If biomolecules could be caused to migrate within the RTIL, this could present potential enhancements in ME-SIMS measurements. Biomolecules could be forced to concentrate at the surface of the RTIL, where SIMS makes its measurement. Furthermore, the possibility of discriminating

which biomolecules were measured could also be realized.

10 Acknowledgements

I would like to thank the Charles Center for their grant support. I would like to thank Dr. William Cooke for his guidance on this project. In addition, I would like to thank Peter Harris for his aid in both the 2,5 DHB and RTIL work. Finally, I would like to thank the W&M staff at the Applied Research Center in Newport News, VA for the use of their facilities.

11 Glossary of Terms

MALDI Matrix Assisted Laser Desorption Ionization. A mass analysis technique which places analyte molecules within a matrix and uses a laser to ablate molecules from the surface of the sample.

ME-SIMS Matrix Enhanced Secondary Ionization Mass Spectrometry. A mass analysis technique which combines the SIMS analysis with MALDI sample preparation protocol.

RTIL Room Temperature Ionic Liquid. An ionic liquid which has such favorable properties as a wide ranging thermal stability and negligible vapor pressure.

SIMS Secondary Ionization Mass Spectrometry. A mass analysis technique where energetic primary ions bombard the surface of a sample causing secondary ions to be sputtered from the surface.

ToF-SIMS Time of Flight Secondary Ionization Mass Spectrometry. A SIMS technique that uses a time of flight mass analyzer.

References

[1] D.I. Malyarenko *et al.*, *Applied Surface Science*, **231-232**, 357-361 (2004).

[2] Liam A. McDonnell *et al.*, *Anal. Chem.*, **75**, 4373-4381 (2003).

[3] http://www.eaglabs.com/cai/simstheo/effects.htm

[4] Mark A. Ray *et al.*, *Hanbook of Instrumental Techniques for Analytical Chemistry*, "Secondary Ion Mass Spectrometry".

[5] A. Delcorte and B. J. Garrison, *J. Phys. Chem. B*, **104**, 6785 (2000).

[6] K. J. Wu and R. W. Odom, Anal. Chem. **68**, 873 (1996).

[7] Robert J. Cotter, *Time-of-Flight Mass Spectrometry*, American Chemical Society, Washington, DC, 1997.

[8] I. Fournier, C. Marinach, J.C. Tabet, and G. Bolbach, *J. AM. Soc. Mass Spec.*, **14**, 893 (2003).

[9] B.J. Garrison *et al.*, App. Surf. Sci. **203/204**, 69 (2003).

[10] J. Kampmeier, K. Dreisewerd, M. Schürenberg, and K. Strupat, *Int. J. Mass Spec.*, **169/170**, 31 (1997).

[11] Zhaoyang Liu and Kevin L. Schey, *J Am Soc Mass Spectrom*, **16**, 482 490, (2005).

[12] M. Zabet-Moghaddam *et al.*, *Rapid Commun. Mass Spectrum*, **18**, 5151-148, (2002).

[13] L. Cohen, A. Busev, *Anal. Bioanal. Chem*, **373**, 571, (2002).

[14] Y. Li, *et al.*, *J Am. Soc. Mass Spectrom.*, **16**, 679-682, (2005).

[15] J. Jones et al., *J Am. Soc. Mass Spectrom*, **16**, 2000-2008, (2005).

[16] "Ionic Liquids", *Organic Chemistry Portal*, http://ww.organic-chemistry.org/topics/ionic-liquids.shtm, (current April 4, 2006).

[17] Scanning Probe Microscopy Training Notebook, Digital Instruments, Veeco Metrology Group.